Miner Deposita
DOI 10.1007/s00126-007-0125-7

ARTICLE

The structural controls of gold mineralisation within the Bardoc Tectonic Zone, Eastern Goldfields Province, Western Australia: implications for gold endowment in shear systems

Anthony A. Morey · Roberto F. Weinberg · Frank P. Bierlein

Received: 27 July 2005 / Accepted: 5 January 2007

Abstract The Bardoc Tectonic Zone (BTZ) of the late Archaean Eastern Goldfields Province, Yilgarn Craton, Western Australia, is physically linked along strike to the Boulder-Lefroy Shear Zone (BLSZ), one of the richest orogenic gold shear systems in the world. However, gold production in the BTZ has only been one order of magnitude smaller than that of the BLSZ (~100 t Au vs >1,500 t Au). The reasons for this difference can be found in the relative timing, distribution and style(s) of deformation that controlled gold deposition in the two shear systems. Deformation within the BTZ was relatively simple and is associated with tight to iso-clinal folding and reverse to transpressive shear zones over a <12-km-wide area of high straining, where lithological contacts have been rotated towards the plane of maximum shortening. These structures control gold mineralisation and also correspond to the second major shortening phase of the province (D_2). In contrast, shearing within the BLSZ is concentrated to narrow shear zones (<2 km wide) cutting through rocks at a range of orientations that underwent more complex dip- and strike-slip deformation, possibly developed throughout the different deformation phases recorded in the region (D_1–D_4). Independent of other physico-chemical factors, these differences provided for effective fluid localisation to host units with greater competency contrasts during a prolonged mineralisation process in the BLSZ as compared to the more simple structural history of the BTZ.

Keywords Yilgarn Craton · Western Australia · Orogenic gold · Deformation · Shear zones · Late Archaean

Editorial handling: G. Beaudoin

A. A. Morey
predictive mineral discovery*Cooperative Research Centre, Australian Crustal Research Centre, School of Geosciences, Monash University,
PO Box 28E, Melbourne, VIC 3800, Australia

R. F. Weinberg
Australian Crustal Research Centre, School of Geosciences, Monash University,
PO Box 28E, Melbourne, VIC 3800, Australia

F. P. Bierlein
Tectonics Special Research Centre,
School of Earth and Geographical Sciences,
University of Western Australia,
35 Stirling Highway,
Crawley, WA 6009, Australia

F. P. Bierlein (✉)
Centre for Exploration Targeting (M006),
School of Earth and Geographical Sciences,
University of Western Australia,
35 Stirling Highway,
Crawley, WA 6009, Australia
e-mail: fbierlein@tsrc.uwa.edu.au

Introduction

The late Archaean Eastern Goldfields Province (EGP) of the Yilgarn Craton, Western Australia, is a globally significant orogenic lode gold province, with one giant (>250 t Au) and at least 15 world-class (>100 t Au) gold camps or deposits (e.g. Hagemann and Cassidy 2000; Goldfarb et al. 2001). These deposits are associated with first-order regional shear zones and are commonly sited on second- or third-order faults that splay off these first-order structures (e.g. Groves et al. 1987; Eisenlohr et al. 1989). Past studies and reviews on this style of gold mineralisation (e.g. Robert and Poulsen 1997; Hagemann and Cassidy

2000, 2001; Brown et al. 2002; Baggott et al. 2005) have focussed on systems that host the larger (>100 t Au) gold systems, with smaller gold deposits being underrepresented within the literature. A very useful approach to understand the processes that control gold endowment of an orogenic terrane is to compare the nature of shear systems that are richly endowed with those that are not. The approximately 80-km-long Bardoc Tectonic Zone (BTZ, Fig. 1) is one such shear system that only hosts small deposits. It produced ~100 tonnes of gold from more than 80 recent and historic deposits, summarised in Witt (1992). Deformation and mineralisation styles for the BTZ are characterised here by studying three representative deposits of the BTZ (Fig. 1) and then comparing these results to the well-researched and connecting Boulder-Lefroy Shear Zone (BLSZ, e.g. Ridley and Mengler 2000; Bateman and Hagemann 2004; Cox and Ruming 2004; Weinberg et al. 2005) and other major examples worldwide. This compar-

Fig. 1 Geological map of a portion of the Eastern Goldfields Province, showing the relatively broad Bardoc Tectonic Zone (*centre—line in red*), its flanking granitic domes and relevant field localities. Part of the Boulder-Lefroy Shear Zone (*blue*) is also shown. Inset: study area relative to Western Australia. Modified after Swager and Griffin (1990a)

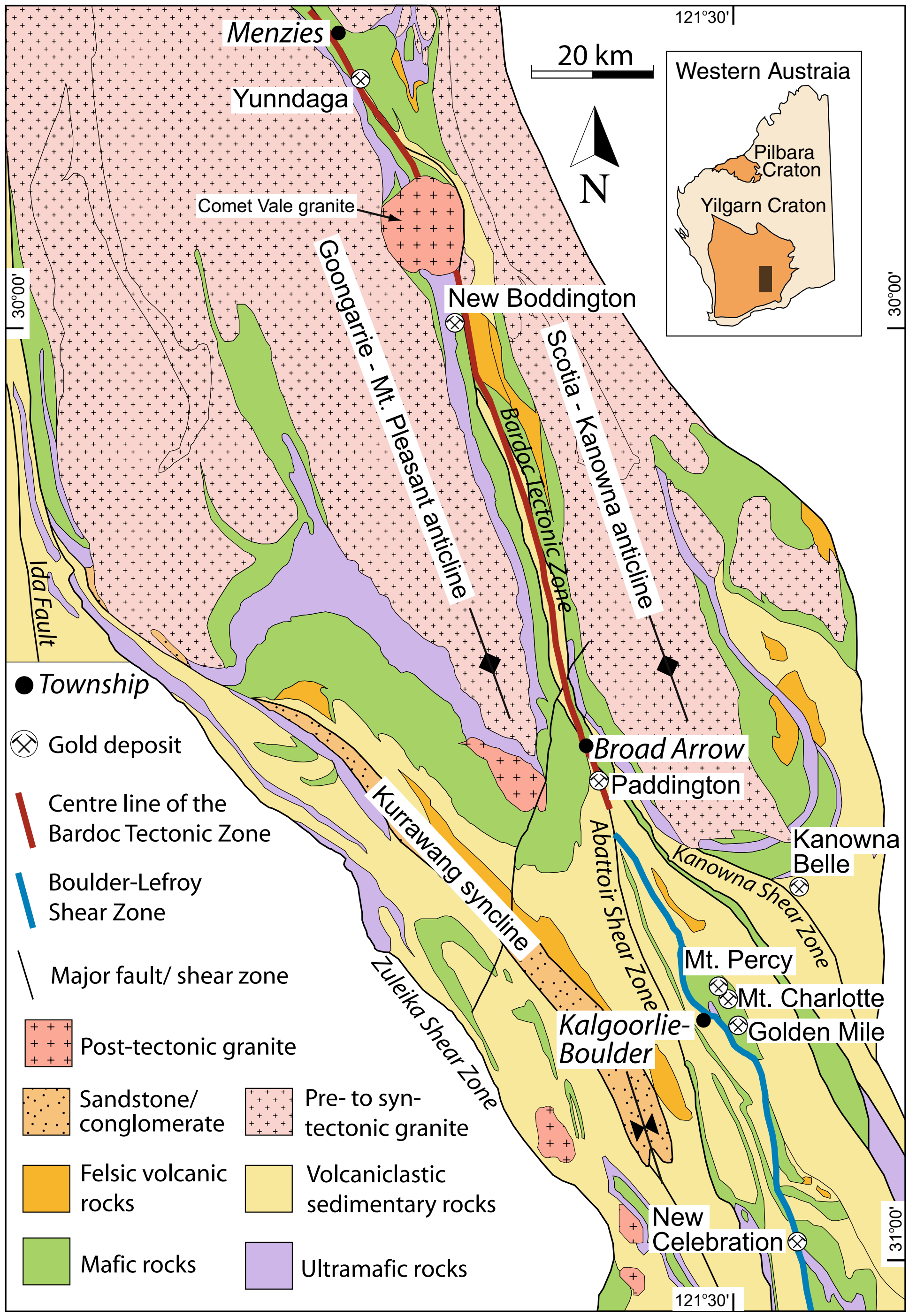

ison highlights key structural features that help account for differences between well-endowed (e.g. BLSZ) and moderately endowed shear systems (e.g. BTZ), typical of Archaean greenstone terranes.

Geological framework

Approximately 70% of the Archaean Yilgarn Craton is composed of metamorphosed granitoid rocks with the remainder comprising metamorphosed felsic to ultramafic volcanogenic rocks (termed greenstones) and banded iron formations. Relatively high-grade granite–gneiss units (approximately 3.73 Ga) dominate the western parts of the craton, whereas greenschist-facies units as young as 2.55 Ga prevail towards the eastern part of the craton (Myers 1993). The EGP covers approximately the eastern third of the Yilgarn Craton, where the majority of gold deposits are located (Hagemann and Cassidy 2001).

The Yilgarn Craton has been divided into a number of tectonic provinces, terranes and domains, which are demarcated by their differing rock types, ages, metamorphic grades and tectonic histories (Williams 1974; Gee 1975; Myers 1993; Swager et al. 1995; Swager 1997). Whitaker and Bastrakova (2002) have divided the Yilgarn Craton into geophysical provinces based on the delineation of regional aeromagnetic domains. These boundaries are defined by major faults and shear systems and, especially within the EGP, have a dominant NNW trend. Greenstone units and granites also dominantly strike towards NNW.

Within the approximately 2.72 to 2.60 Ga southern EGP, the greenstones are divided into a lower basalt unit, overlain by komatiite, upper basalt, volcanogenic sedimentary rocks and unconformable fluvial quartzo-feldspathic units (Witt 1993; Swager 1997). A number of mafic intrusive rocks (dolerites and gabbros) have also been emplaced into these successions (Witt 1993, 1994). A regional four-phase contractional deformation history has been constructed for the EGP, occurring between approximately 2.675 and 2.620 Ga (Swager 1997). Details of this deformation scheme are outlined in Table 1. The earliest shortening event (D_1) is characterised by ~N-directed thrusting and recumbent folding that resulted in large-scale repetition of the greenstone sequences, clearly defined south of Kalgoorlie-Boulder (Gresham and Loftus-Hills 1981; Swager and Griffin 1990b; Fig. 1). This was followed by a major phase of ENE–WSW shortening (D_2), which

Table 1 Details of regional shortening and gold mineralisation events within the Eastern Goldfields Province

Event and timing constraints (Ma)	Description	Localities, see Fig. 1	Gold mineralisation associated with the Boulder Lefroy Shear Zone
D_1 Pre-2681±5	Subhorizontal thrusting and recumbent folding	Kalgoorlie to south of Kambalda (not in Fig. 1) Subhorizontal granite–greenstone contacts	
D_2 Post-c. 2675	Upright regional folds with NNW-trending axial planes and shallowly plunging fold axes	Kambalda anticline (not in Fig. 1) Goongarrie-Mount Pleasant anticline Scotia Kanowna anticline Kurrawang syncline	D_1 or early D_2 Fimiston lodes Cross-cutting D_2 Oroya lodes (Kalgoorlie)
D_3 Post-c. 2660	Sinistral strike-slip on NNW-trending shear zones, and continued regional shortening; sub vertical movements on some shear zones during late D_3	Boulder-Lefroy Shear Zone Zuleika Shear Zone	New Celebration Kambalda-Saint Ives
D_4 Pre-c. 2620	Dominantly dextral movements on NNE-trending shear zones	Kalgoorlie Paddington Mount Pleasant (Ora Banda)	Mount Charlotte (Kalgoorlie)

Adapted from Swager and Griffin (1990b), Witt (1993), Swager (1997), Nguyen et al. (1998), Ridley and Mengler (2000), Bateman and Hagemann (2004), and Weinberg et al. (2005)

gave rise to NNW-trending regional upright folds and major reverse faulting/thrusting that defines much of the present-day architecture of the EGP (e.g. Passchier 1994; Swager et al. 1995; Swager 1997; Weinberg et al. 2003; Davis et al. 2007). This deformation episode occurred between approximately 2.650 (Hammond and Nisbet 1992) and 2,660 (Swager 1997), or from 2,655 onwards (Weinberg et al. 2003), and was associated with multiple shortening episodes (Davis et al. 2001) and intervening extensional phases (Davis and Maidens 2003; Blewett et al. 2004). Further ENE–WSW shortening reactivated NNW-trending D_2 structures to produce dominantly sinistral strike-slip ductile faults (D_3, e.g. Swager et al. 1995; Chen et al. 2001a). This was followed by brittle–ductile NE-tending dextral and NW-trending sinistral faulting (D_4). The major stages of orogenic gold mineralisation within the EGP took place during the later stages of deformation (D_3–D_4, e.g. Groves et al. 2000). Regional studies on intrusive rocks by Yeats et al. (1999) and Yeats et al. (2001) concluded that gold mineralisation, broadly constrained between approximately 2,680 and 2,625 Ma, occurred diachronously in different parts of the EGP; however, the major gold mineralisation event for the EGP has been further constrained to approximately 2,640 and 2,630 Ma (Groves et al. 2000), with evidence for an earlier mineralisation episode within the Laverton greenstone belt occurring between approximately 2,655 to 2,650 Ma (Brown et al. 2002; Salier et al. 2004, 2005).

Overview of the BTZ

The BTZ is a NNW-tending corridor of highly strained supracrustal rocks situated between two elongate granitic bodies known as the Scotia-Kanowna and Goongarrie-Mt. Pleasant domes (Fig. 1). These domes are regarded as pre- to syn-D_2 antiformal structures, and the BTZ likely represents the sheared-out synclinal sequence that separates these two regional structures (Witt and Swager 1989; Witt 1994). Beeson et al. (unpublished) reported that units within the BTZ are partitioned into narrow high-strain shear zones and relatively wider, synclinal low-strain zones, inferring that the high-strain zones are sheared off anticline hinges separating synclines. The BTZ is also the boundary structure between two tectono-stratigraphic sequences: the Ora Banda Domain to the west and the Boorara Domain to the east (Swager et al. 1995).

Rock units within the BTZ include peridotites, komatiites, high-Mg and tholeiitic basalts, ultramafic to mafic intrusive sills, rare felsic intrusive bodies, shales and felsic to intermediate volcanogenic sedimentary rocks. Along strike, these units are strained and attenuated; however, some units can be traced continually for more than 100 km (Witt 1994). The relatively small (~5×10 km) and circular Comet Vale granite also lies within the tectonic zone (Fig. 1). Regional aeromagnetic images show that this granite is made up of undeformed structures, suggesting it is a post-tectonic intrusive body that truncates the NNW-trending fabric of the BTZ (Witt 1993). The BTZ splays into a number of regional shear zones towards the south, which includes the Kanowna, Boulder-Lefroy, and Abattoir Shear Zones. These splays occur where the narrow corridor between the bounding granitic domes opens up into a broad and less-deformed zone of supracrustal rocks (Fig. 1). In the Menzies region in the north, the strike of the BTZ changes from a NNW trend to a NW trend (Witt 1993; Swager 1997; Hodkiewicz et al. 2005).

A number of reports have previously described individual gold deposits along the BTZ (Booth, unpublished; Bottomer and Robinson 1990; Colville et al. 1990; Hancock et al. 1990; Ransted 1990). However, regional overviews of deformation and gold mineralisation are limited to Witt (1992, 1993) and unpublished exploration reports (Beeson et al., unpublished; Manly, unpublished). From these reports, all types of rock units exposed within the BTZ can potentially host gold mineralisation, but as with most of the EGP, the majority of past gold production has been derived from relatively competent mafic extrusive or intrusive units. Styles of gold mineralisation within the BTZ range from brittle to ductile, vein-dominated ore bodies that are located dominantly within, or at the margin of, the relatively more competent units (Witt 1993). Towards Menzies, mineralisation is progressively more ductile as the metamorphic conditions recorded by rocks hosting gold change from greenschist to lower-amphibolite facies (Beeson et al., unpublished), a pattern consistent with the continuum model of Groves (1993).

There are limited geochronological data constraining the absolute timing of host rock extrusion/intrusion, structural deformation or gold mineralisation within the BTZ. A granophyre dike, approximately 20 km NNW of the Paddington Deposit, yielded a formation age of 2,661±3 Ma (Nelson 1998). An emplacement age for the Scotia-Kanowna Dome bounding the BTZ on its eastern side (Fig. 1) was determined by a U–Pb zircon sensitive high-resolution ion microprobe (SHRIMP) age to be 2,657±5 Ma (Nelson 2002). This can be interpreted as a maximum age for D_2 as the Scotia Kanowna Dome is interpreted as a pre- to syn-tectonic intrusive dome. Overprinting relationships and SHRIMP U–Pb studies on felsic porphyries within the Kanowna Belle Deposit to the east of the BTZ (Ross et al. 2004, Fig. 1) yielded a similar maximum D_2 age of 2,655±6 Ma.

Gold mineralisation was inferred by Witt (1993) to be associated with relatively late strike-slip D_3 or D_4 structures. Beeson et al. (unpublished), in contrast, reported that the bulk of gold mineralisation within the BTZ is hosted within relatively early, compressional or transpressional D_2 structures, and that later strike-slip structures are only a minor host to economic gold mineralisation. This study attempts to further resolve the relative structural timing of gold mineralisation within the BTZ, and compare these results with published data from other shear systems within the EGP, especially the connected BLSZ.

Paddington gold deposit

Geological setting

Paddington is the largest known gold deposit within the BTZ, and it is located approximately 35 km NNW of Kalgoorlie-Boulder, close to where the BTZ splays southwards into the Abattoir, Boulder-Lefroy and Kanowna Shear Zones (Fig. 1). The open pit is divided into a northern and a southern section, which are offset by a series of NE-trending brittle-dominated faults (Fig. 2). The northern Paddington pit is partially obscured by mine tailings. Between 1998 and 2000, 18 tonnes of ore was mined averaging 2.28 g/t Au, or ~37 t of gold (Sheehan and Halley, unpublished). A number of other open-pit gold deposits have been mined within the greater Paddington area, including four open pits within the Broad Arrow area, ~5 km to the north (Fig. 1).

Rock units at Paddington trend NNW and dip steeply to the east and west. The lowest stratigraphic unit is an ultramafic unit, dominated by foliated talc–chlorite–carbonate schists, with minor spinifex and fragmental komatiite rocks (Fig. 2). Overlying the ultramafic sequence are two tholeiitic basalt units and a leucoxene-bearing dolerite sill (Paddington Dolerite; Sheehan and Halley, unpublished). A less extensive, leucoxene-free dolerite lens also exists within the central portion of the deposit. A number of highly strained sulphidic carbonaceous shales occur at the contact of the mafic units, or as interflow units within the basalt (Hancock et al. 1990). A thick unit of volcanogenic sedimentary shales and sandstones (regionally known as the Black Flag Group; e.g. Hunter 1993) is the highest stratigraphic unit (Fig. 2).

Gold mineralisation and associated veins are mainly hosted within the more competent dolerite and basalt units (Fig. 2). Throughout the deposit, two major types of gold-bearing veins exist: (1) a steeply-dipping, laminated vein that is up to 3 m wide and runs continuously along the strike of the open pit (~1.2 km in length), and (2) a series of sub-horizontal and stacked ladder veins (Alardyce and Vanderhor 1998; Sheehan and Halley, unpublished), which were described as 'stockworks' by Hancock et al. (1990). These structures are further described below.

Local deformation and gold mineralisation events

The first local deformation phase at Paddington is characterised by a NNW-trending foliation (Fig. 2) that overprints primary bedding surfaces (S_0). This foliation is associated with steeply dipping stretching lineations, and both of these structures are more intensely developed within the less competent sedimentary and ultramafic units as well as near the margins of the more competent mafic units. This foliation is axial planar to tight to iso-clinal upright folds (Fig. 3a). Within all units, reverse and thrust faults strike between 315° and 350°. These faults have sub-metric offsets, cross cut the iso-clinal upright folds (Fig. 3b) and also indicate ENE-WSW shortening. Consistent with multiple local shortening events described in Davis et al. (2007), all of these structures indicate an intense ENE-WSW shortening episode and can be directly correlated with the regional D_2 deformation phase described in Table 1.

A major steep reverse D_2 shear zone within the mafic unit hosts the laminated vein. The margins of this vein are characterised by alternating laminations of wall rock and quartz–carbonate vein material (Fig. 3c–e). Similar to S_0 and S_2, this vein strikes NNW but dips vertically or steeply towards the east. Wall-rock alteration, as much as 1 m outward from the laminated vein, is characterised by carbonate–quartz–muscovite–sulphide–gold assemblages. The sulphides are dominated by arsenopyrite, with lesser amounts of pyrite + chalcopyrite + galena ± sphalerite (Booth, unpublished; Hancock et al. 1990; this study).

At the margins of the laminated vein (Fig. 3c), steeply plunging stretching lineations along C-planes and associated S–C fabrics imply reverse dip-slip movement (Fig. 3d,e). Rotated and fractured arsenopyrite grains and associated pressure shadows also indicate reverse movement parallel to the stretching lineation. Visible gold is located within arsenopyrite fractures (Fig. 3f), which are restricted to the alteration haloes of the laminated veins. Like the vein itself, the alteration halo and its deformation, including the fracturing of arsenopyrite are also most likely due to the progressive ENE–WSW D_2 (cf. Hodgson 1989; Robert and Poulsen 2001).

The flat-lying ladder veins are generally 1 to 5 cm thick (locally as much as 30 cm thick, Fig. 4a), and like the laminated vein, wall rock alteration is characterised by carbonate–quartz–sericite–sulphide–gold assemblages, which extend <20 cm on either side of the vein margins (Fig. 4b). Consistent with the laminated lode, the sulphides proximal to the ladder veins are dominated by arsenopyrite with accessory pyrite + sphalerite ± galena. Unlike the

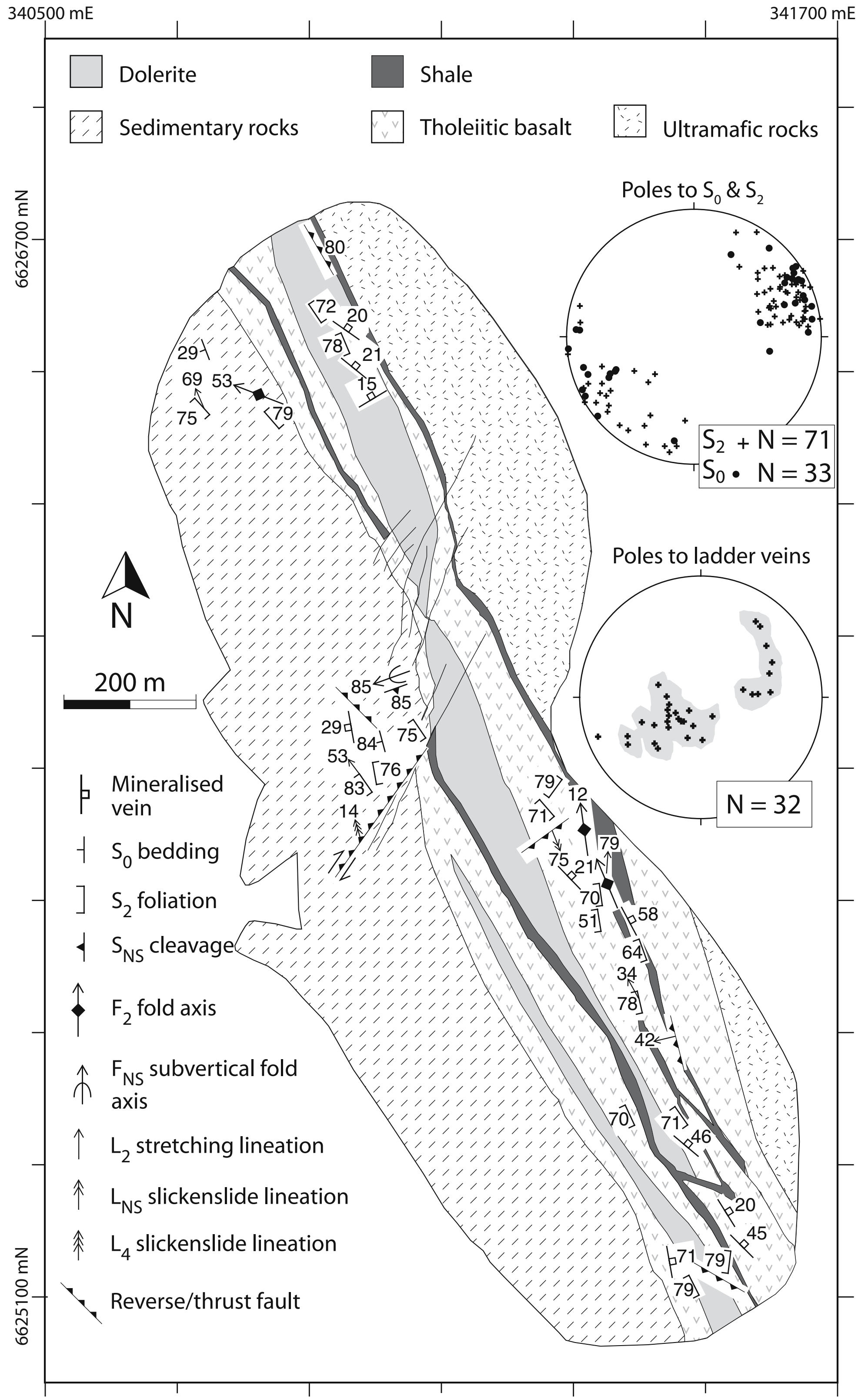

Fig. 2 Geological map of the Paddington open pit with representative structural measurements. Lithological units adapted from Sheehan and Halley (unpublished). Stereographic projections include poles to bedding planes of sedimentary units, and poles to planes of S_2 and extensional ladder veins

shear-related laminated vein, the shallowly dipping ladder veins are planar and extend for tens of metres in a ~N–S direction (Fig. 4a). They are generally oriented at a high angle to the steep NNW-trending D_2 axial planar foliation and lineation, indicative of extensional vein array-type structures (cf. Fig. 16 in Robert and Poulsen 2001).

The poles to the ladder veins define two broadly distributed clusters (Fig. 2), which most likely represent a

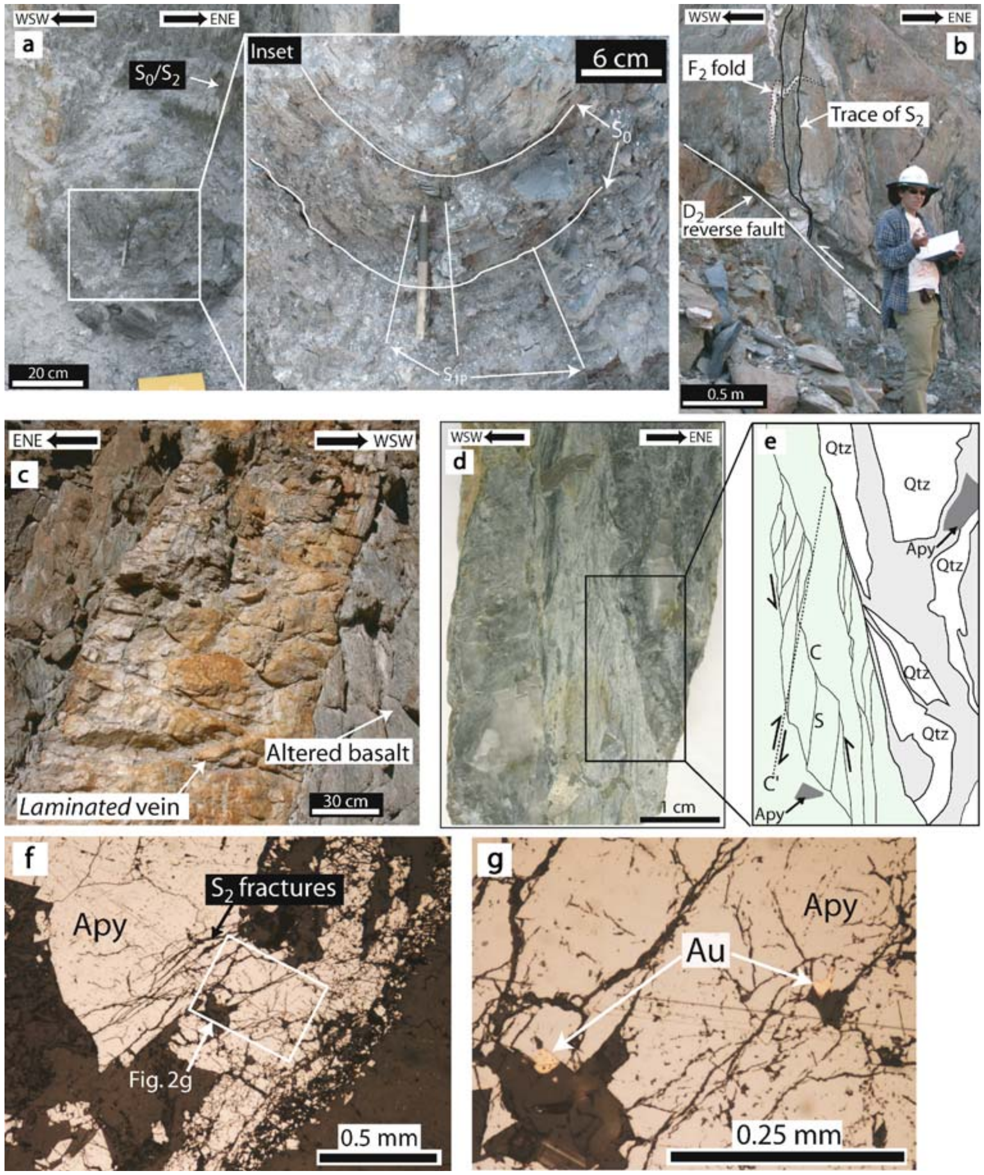

Fig. 3 Representative D_2 structures and the laminated vein from the Paddington deposit. **a** Photograph of an F_2 fold hinge, panned out and close up showing iso-clinally folded S_0 layers. **b** Photograph of a NNW-tending reverse/thrust fault and folded unmineralised vein associated with D_2. **c** Photograph of the laminated vein and hosting foliated basaltic rock from the southern part of the Paddington open pit. Note the vein margins, where alternating selvages of wall rock and vein minerals occur. **d** Close up of the margin of the laminated vein showing the characteristic wall rock selvages and vein laminations. **e** Trace of the laminated vein selvages, showing shear sense indicators and arsenopyrite (*Apy*) quartz (*Qtz*) veins and muscovite (*green*) and quartz-dominated (*grey*) alteration selvages. **f** Reflected light photomicrograph of the wall rock alteration halo associated with the laminated vein showing the fractured nature of the arsenopyrite (*Apy*) grains. Mineral abbreviations used in all figures follow Kretz (1983). **g** Close-up of **f**, showing native gold grains distributed along arsenopyrite (*Apy*) grain boundaries and fractures

conjugate pair. The wide variation in attitude within these clusters might represent local and complex variations in stress orientation during vein formation. The conjugate ladder veins are not folded, but quartz in the veins are re-crystallised and define a faint foliation parallel to S_2, or mutually cross cut or overprinted by the S_2 foliation (Fig. 4c). Considering the veins as a conjugate pair, an ENE–WSW sub-horizontal shortening axis and vertical extensional axis can be inferred. This is essentially the same shortening axis inferred for D_2-related structures, and because these veins are mutually overprinted by or cut across S_2, we conclude that they also formed during D_2.

The structural and overprinting relationships described above indicate that the laminated and ladder veins are controlled by the same deformation event (D_2). This is remarkably similar to gold bearing veins at the Beaufor

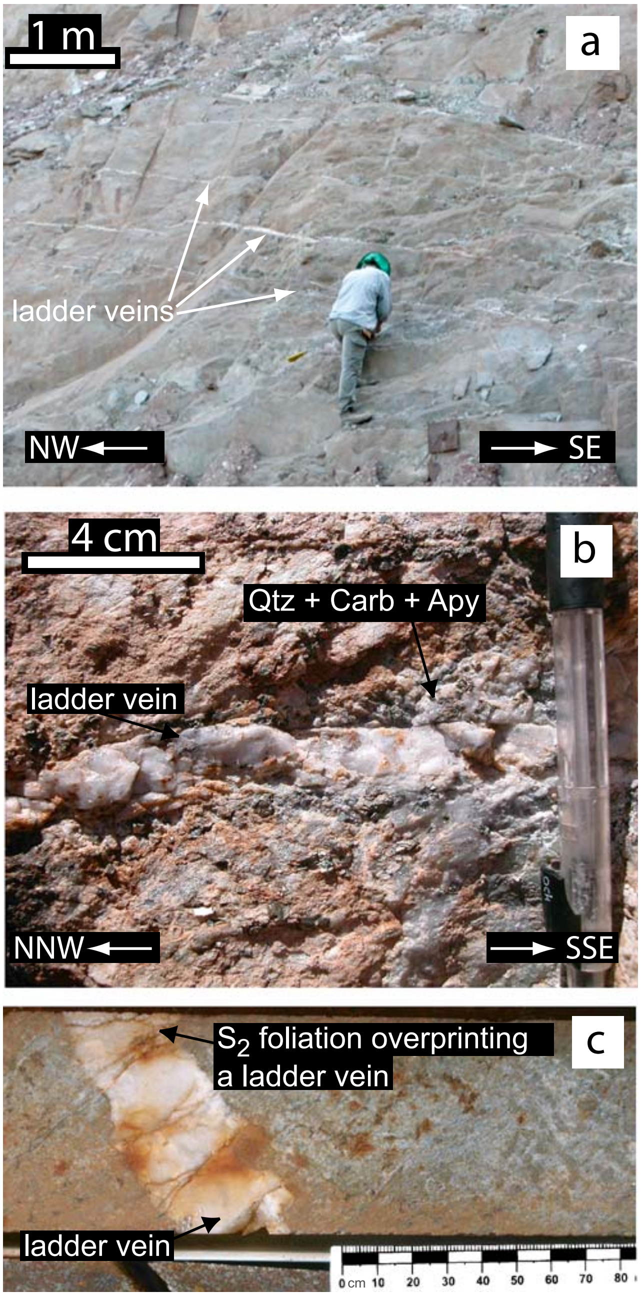

Fig. 4 Representative images of the ladder veins from the Paddington deposit. **a** Pit wall photograph showing the nature of the fine (generally <5 cm thick) ladder veins hosted within the dolerite unit. **b** Close-up of a quartz–carbonate ladder vein showing its associated quartz- (*Qtz*), carbonate- (*Carb*) and arsenopyrite- (*Apy*) dominated wall rock alteration assemblage. **c** Diamond drill core intersection of a mineralised ladder vein cross-cut by S_2 foliation

(formerly Perron or Pascalis Nord) and Sigma mines, Abitibi greenstone belt, Canada, where shear-related fault-fill and relatively later conjugate extensional veins were interpreted to have progressively formed during the one deformation event (Ames 1948; Hodgson 1989; Robert and Brown 1986; Gaboury et al. 2001; Tremblay 2001).

Post-mineralisation deformation

In the central part of the Paddington open pit, steeply plunging, sub-vertical open folds refold S_0 and S_2 planes (Fig. 2). These folds trend between 070° to 085° and fold axes dip steeply WSW (Fig. 5a,b). These structures define a second local deformation phase and a maximum shortening axis oriented NNW–SSE. These structures are poorly developed, restricted to localised areas of the Paddington pit and thus most likely represent a local deviation of regional stresses occurring between D_2 and D_4 (termed D_{NS}, Fig. 5c).

Within the southern part of the Paddington pit, D_2 ladder veins are offset by reverse faults that trend between 225°/68°S and 239°/64°S. Quartz–carbonate veins infill these late faults, but in contrast to the laminated and ladder veins, no sulphide or gold assemblages are associated with these unmineralised structures. Similar to the steeply plunging open folds (above), slickenslide measurements along fault surfaces (75°–157°, 70°–171°) and associated *en echelon* tension veins suggest localised sub-horizontal NNW–SSE shortening (Figs. 2 and 5d). These reverse faults likely formed during the same local deformation event as the steeply plunging second generation of folds, as they have similar inferred shortening axes and relative timing relationships.

The last deformation event at Paddington is characterised by a series of steeply dipping 035°- to 045°-trending, brittle–ductile dextral faults that laterally displace the NNW-trending ore-bearing veins by less than 50 m (Fig. 2, Hancock et al. 1990; Alardyce and Vanderhor 1998). The faults drag S_0 and S_2 planes in an oblique fashion and kinematic indicators such as drag folds and slickenslide lineations (Fig. 2) indicate oblique dextral/reverse movement. This event corresponds to the regional D_4 event (Table 1).

New Boddington deposit

Geological setting

The New Boddington gold deposit (Fig. 6) is located approximately 85 km north of Kalgoorlie-Boulder, mid-way between the Paddington deposit and the Menzies township (Fig. 1). The inaccessible Frank's Dam and Hicks Line open pits are situated less than 1 km from New Boddington (Witt 1992) and are part of the same gold camp (Colville et al. 1990). From 1893 to 1942, underground production, mainly centred in what is now the New Boddington open pit, yielded 29,992 t of ore for 0.6 t of gold (Colville et al. 1990). More recent operations from

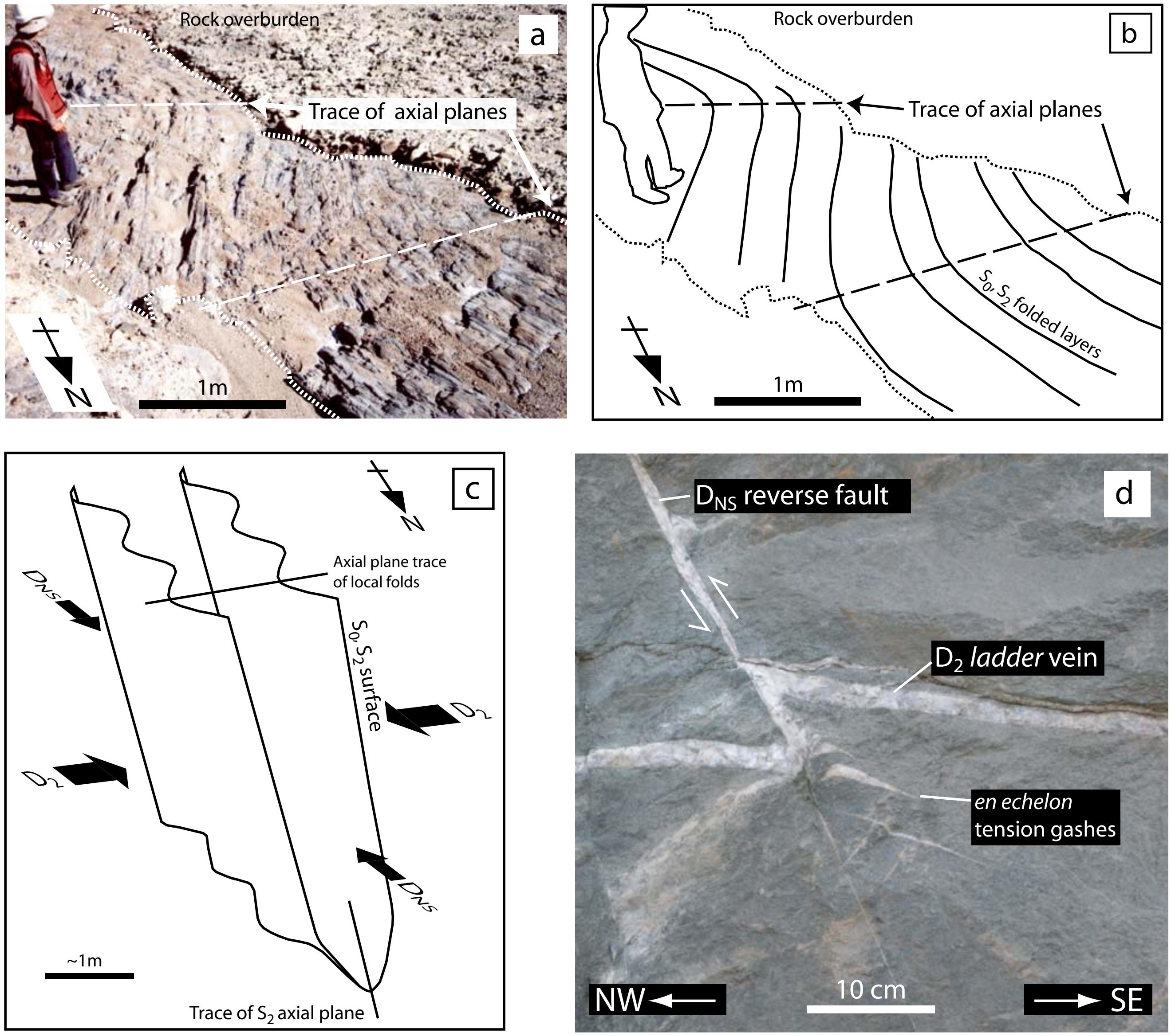

Fig. 5 **a** Oblique photograph and, **b** Corresponding trace of post-D_2, ~N070-trending, sub-vertical open folds within the Paddington pit. **c** Three-dimensional, schematic figure showing the relationship between F_2 and later F_{NS}. **d** Photograph of a vertical rock face showing an ENE–WSW-trending reverse fault overprinting a ladder vein. Note the *en echelon* tension gashes with an apparent asymmetry that also indicates NNW–SSW subhorizontal shortening

1987 to 1989 mined a pre-production resource of 368,240 t of ore for 1.527 t of gold (Witt 1992).

The New Boddington open pit is hosted within a series of ultramafic schists, extrusive and intrusive mafic rocks and an interflow carbonaceous shale (Fig. 6). These units are highly strained and hydrothermally altered, trend NNW and dip steeply to the west. Unit contacts are also defined by strike-parallel shear zones (Fig. 6, Colville et al. 1990). Gold mineralisation is hosted by the mafic units and is associated with stockwork and planar veins cropping out in the western part of the open pit and planar veins in the eastern and central parts of the open pit. Wall rock alteration for both vein types consists of carbonate–quartz–chlorite–biotite–muscovite–arsenopyrite–pyrite–ilmenite–gold assemblages (Morey, in press AJES manuscript). Interpreting that these veins were undeformed Colville et al. (1990) inferred that gold mineralisation was relatively late. Witt (1992) further reported that gold mineralisation was associated with sinistral strike-slip shearing on NNW-trending planes.

Local deformation and gold mineralisation

The earliest deformation event observed in the open pit is characterised by a pervasive NNW-trending foliation that dips steeply to the west. This foliation is strongly developed

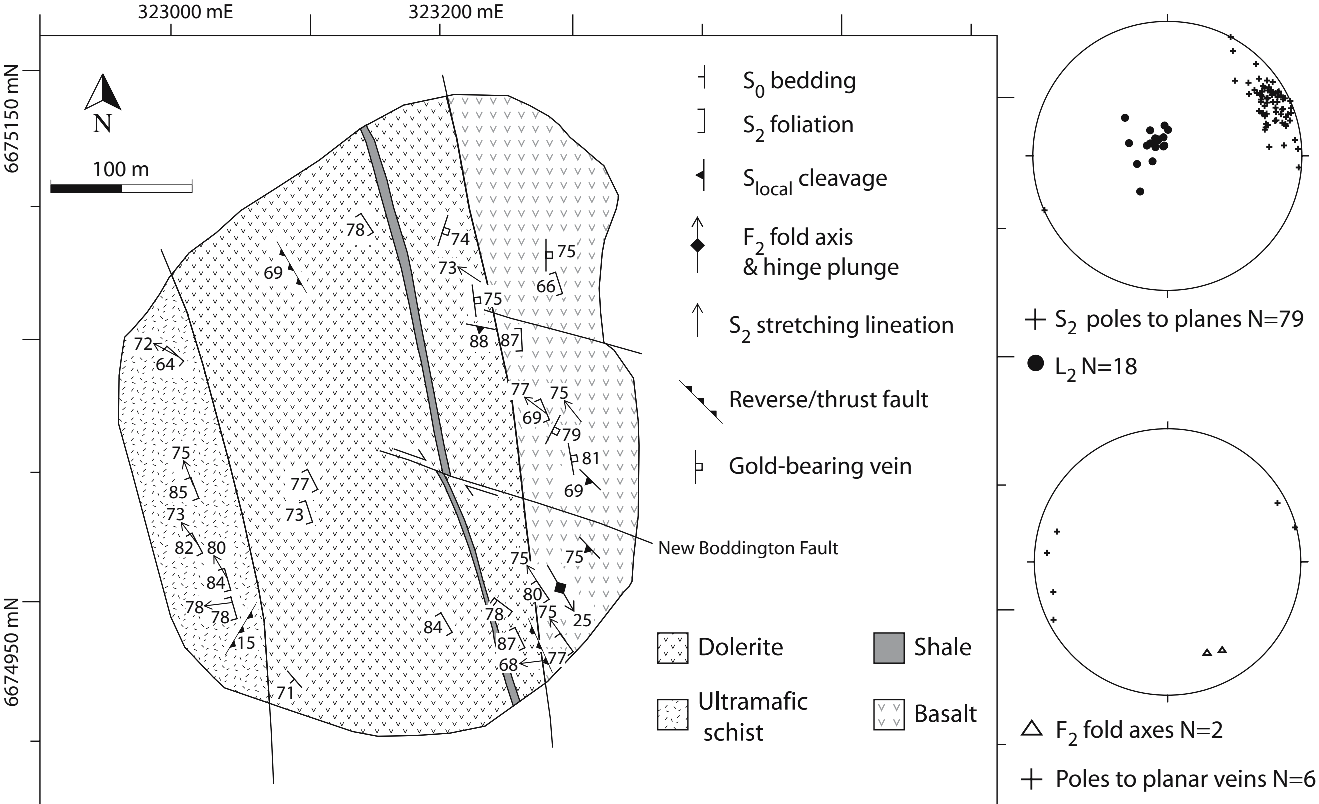

Fig. 6 Geological map of the New Boddington open pit, adapted from Colville et al. (1990), Witt (1992). Lower hemisphere stereonet projections depict poles to planes of the earliest deformation fabric (S_2) and stretching lineations (L_2) along S_2 planes

in all units, and stretching lineations on the foliation planes plunge steeply towards ~315° (Fig. 6). Deformed quartz grains (Fig. 7a) and S-C fabrics observed parallel to the lineation and orthogonal to steep W-dipping foliation planes, consistently indicate reverse movement. Steeply dipping unmineralised quartz veins are iso-clinally folded with axial planes parallel to the dominant NNW-trending foliation (Fig. 7b). Both the shear sense indicators and the folded veins imply that the dominant fabric was associated with sub-horizontal ENE-WSW crustal shortening, which we interpret as being part of the regional D_2 event.

The stockwork veins outcrop in the western part of the open pit but were inaccessible, and out-of-situ stockwork ore blocks were therefore sampled (Fig. 7c). The minor, quartz–tourmaline planar veins are accessible in-situ on the eastern side of the open pit (Fig. 7d). The wall rock alteration zone extends up to 20 cm from both of these structures. The stockwork blocks have a pervasive foliation within the wall rock proximal to these veins (Fig. 7c,e). This foliation is comparable in style and mineralogy to that of the dominant foliation (D_2) in the open pit and is therefore interpreted to represent the structure. Gold-bearing arsenopyrite and lesser pyrite grains proximal to the stockwork veins are fractured and overprinted by the foliation, as revealed by strain shadows surrounding arsenopyrite grains that include gold in fractures (Fig. 7e,f). Given the lack of earlier structures, gold mineralisation is interpreted to have formed during, and subsequently deformed by, this dominant deformation event.

The in-situ planar veins from the eastern section of the open pit were responsible for a small portion of total gold production (Colville et al. 1990). They are 20 to 30 cm

Fig. 7 Collection of deformation and mineralised structures from the New Boddington gold deposit. **a** Photomicrograph parallel to L_2 and perpendicular to S_2 showing a rotated and re-crystallised quartz grain inferring reverse movement associated with the W-dipping S_2 planes. Plane polarised light. **b** Plan view of an iso-clinally folded, unmineralised sub-vertical quartz vein defining an F_2 fold, inferring intense ENE–WSW shortening. **c** Photograph of a mineralised quartz–carbonate (*Qtz–Carb*) stockwork vein. The S_2 foliation is visible as well as arsenopyrite (*Apy*) and chlorite (*Chl*). **d** Photograph of a ~N-trending planar vein that is offset by small scale (<1 m offset) faulting. Inset: photograph of a planar vein boudinaged by S_2. **e** Transmission light photomicrograph of gold bearing arsenopyrite (*Apy*) grains that formed either prior to or during the development of S_2. **f** Backscatter SEM image of a fractured arsenopyrite (*Apy*) grain with visible gold hosted in one of these fractures. Ilmenite (*Ilm*) also occurs as inclusions and within voids within arsenopyrite. **g** Profile view of S_2 planes dragged into local, ~ENE–WSW-trending moderately dipping thrust faults

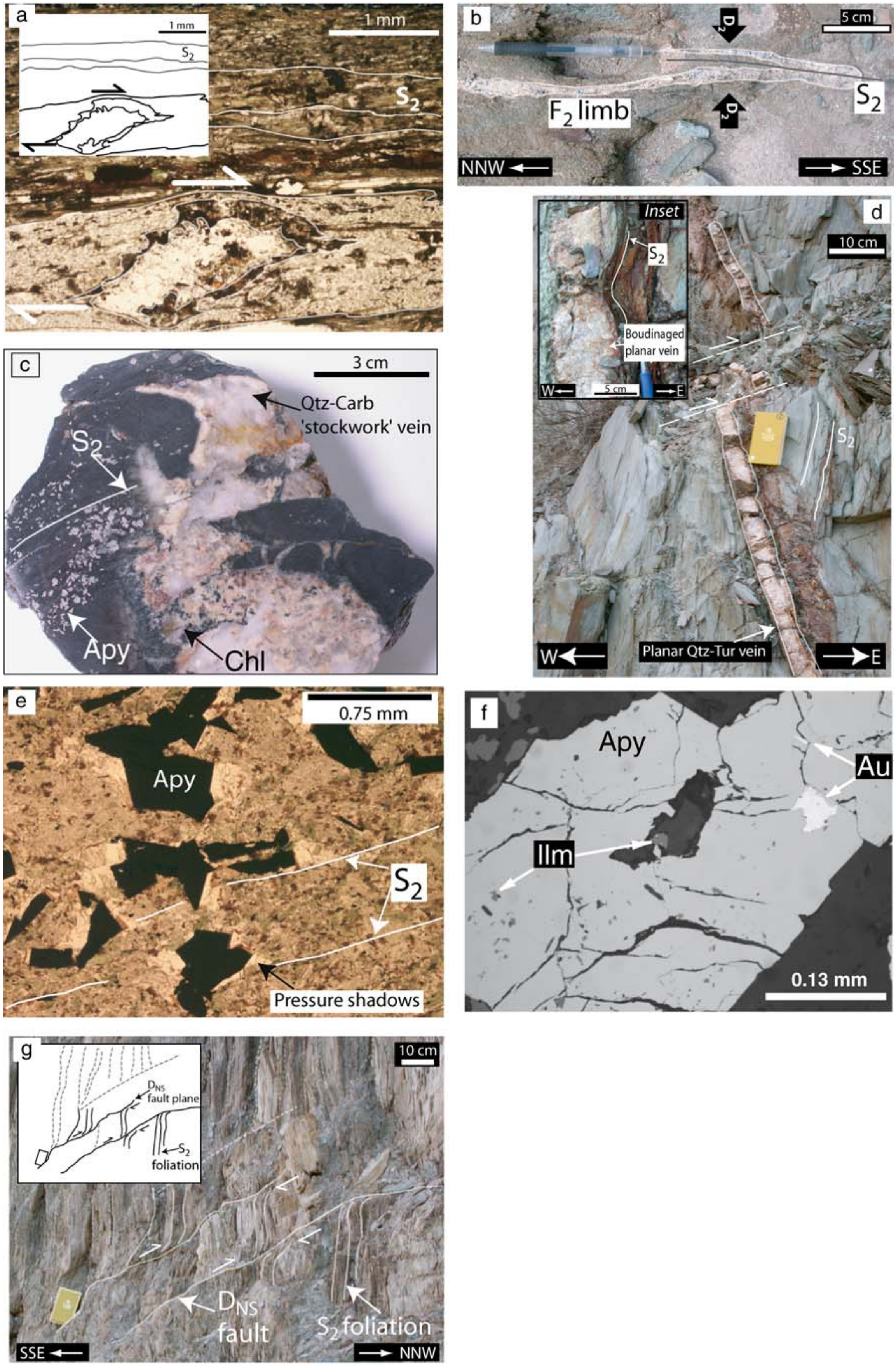
a
1 mm
1 mm
S2
S2
b
5 cm
D2
D2
F2 limb
S2
NNW
SSE
c
3 cm
Qtz-Carb
'stockwork' vein
S2
Apy
Chl
d
Inset
S2
Boudinaged
planar vein
W
5 cm
E
10 cm
S2
W
Planar Qtz-Tur vein
E
e
0.75 mm
Apy
S2
Pressure shadows
f
Apy
Au
Ilm
0.13 mm
g
10 cm
DNS
fault plane
S2
foliation
DNS
fault
S2 foliation
SSE
NNW

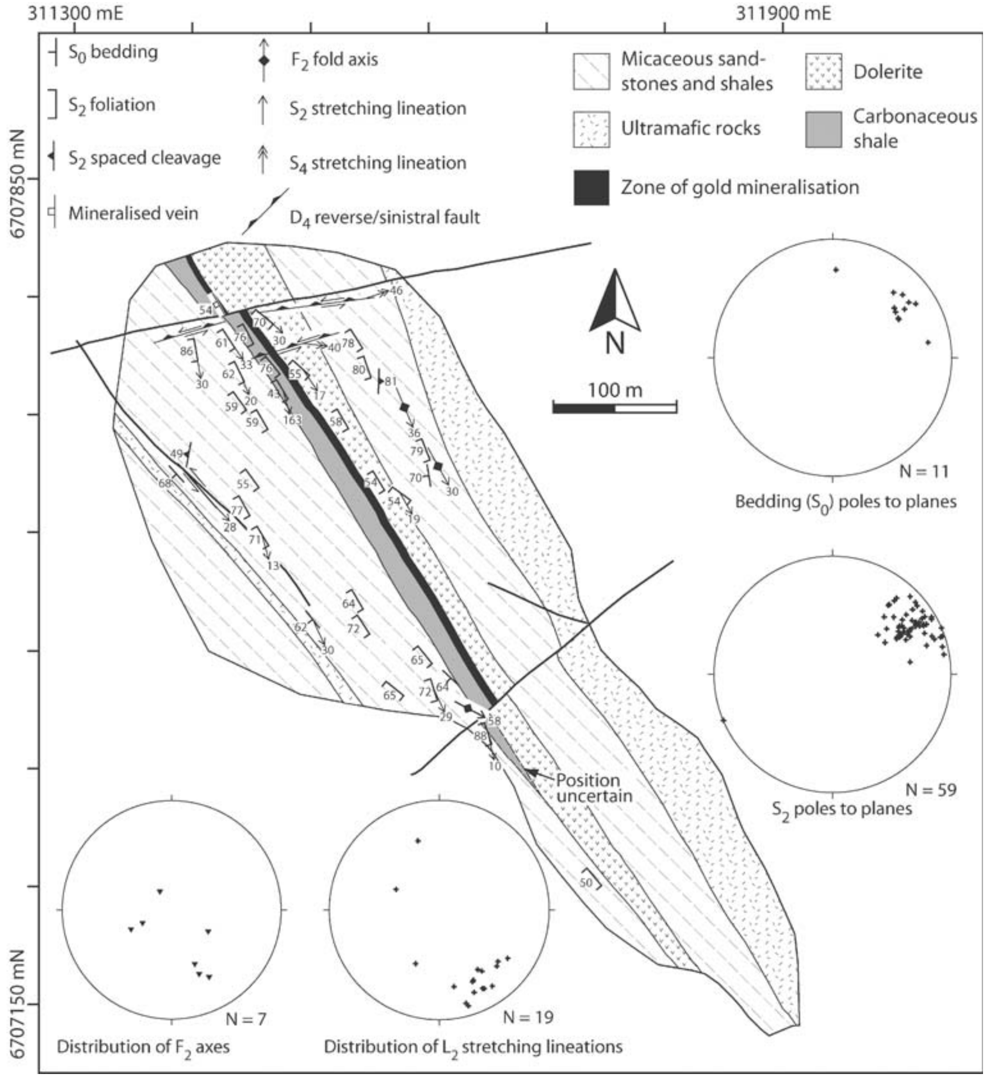

Fig. 8 Geological map of the Yunndaga open pit (after Beeson et al. unpublished) and accompanying stereographic projections representing measured poles to bedding planes (*S_0*) and the initial pervasive fabric (*S_2*) and F_2 fold axes and stretching lineations (*L_2*) associated with S_2. Note that the strike-parallel zone of gold mineralisation corresponds with the contact between the shale and dolerite unit

wide, trend 350° to 360° and dip steeply to the east and west (Figs. 6, 7d). In contrast to unmineralised veins (Fig. 7b), these veins are not significantly deformed, but they are still boudinaged along strike by the S_2 foliation (inset, Fig. 7d). Boudin necks are perpendicular to the L_2 lineation, indicating that boudinage took place during this main deformation phase and are inferred to be contemporaneous with its development.

Post-mineralisation deformation

Within the ultramafic unit, a later deformation event is characterised by brittle–ductile faults with small-scale (<1 m) offsets that trend between 031° and 041°, dip shallowly to moderately to the SE and truncate the major D_2 foliation (Fig. 6). No stretching/slickenslide lineations were identified along these fault planes; however, drag folds on the hanging wall (Fig. 7g) indicate thrusting towards the NW. Similar to the local deformation event at Paddington (D_{NS}, Fig. 5c,d), these small-scale faults define a local shortening event occurring after D_2 with a sub-horizontal shortening axis oriented NNW–SSE. Another set of local faults were observed within the eastern part of the pit (Fig. 7d). These faults trend ~310°, dip steeply to the SW, and offset veins and foliations in a dextral fashion. One of these faults corresponds with the New Boddington fault of Colville et al. (1990; Fig. 6). The isolated nature, brittle–ductile style and similar relative timing and maximum

Fig. 9 Collection of deformation and gold mineralisation images from the Yunndaga gold deposit. **a** Photograph of a moderately plunging, symmetric F_2 fold. **b** Plan view of a sub-vertical asymmetric F_2 fold suggesting a component of strike-slip movement associated with D_2. **c** Plan view of a symmetric sub-vertical F_2 fold with boudinaged limbs, indicating intense ENE–WSW D_2 shortening. **d** Transmission light photomicrograph of a rotated quartz grain with σ-type asymmetrical re-crystallised tails in a plane parallel to L_2 and perpendicular to S_2, which implies sinistral strike-slip shearing. **e** Photograph of a boudinaged, S_2-parallel laminated vein and associated gold-bearing, arsenopyrite-dominated sulfide assemblage. **f** Backscatter SEM image of a fractured arsenopyrite (*Apy*) grain with a fine fracture leading to a gold (*Au*) grain ▶

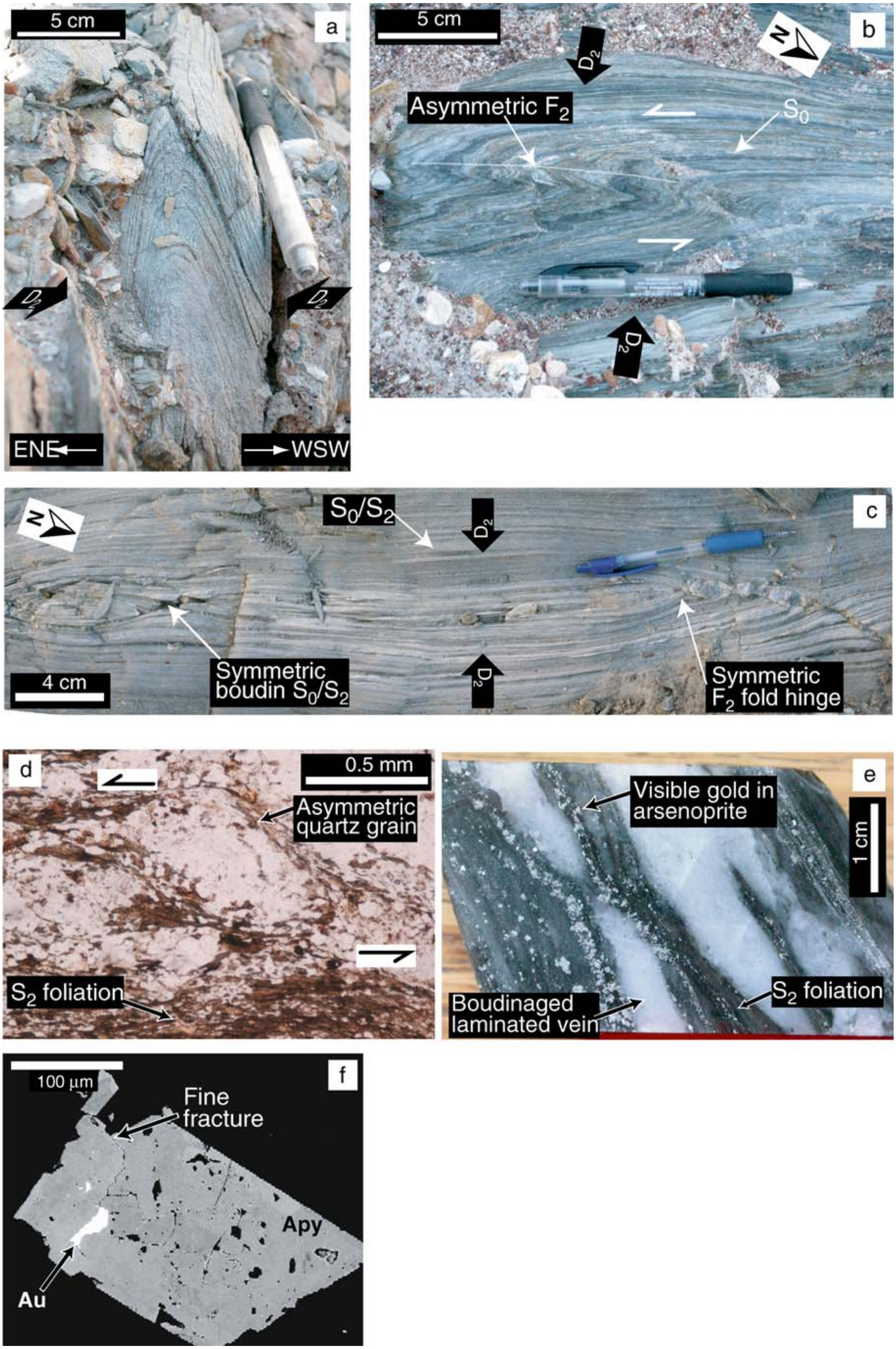
5 cm
a
D2
D2
ENE
WSW
5 cm
b
D2
Asymmetric F2
S0
D2
N
S0/S2
D2
c
N
Symmetric boudin S0/S2
D2
4 cm
Symmetric F2 fold hinge
d
0.5 mm
Asymmetric quartz grain
S2 foliation
e
Visible gold in arsenoprite
1 cm
Boudinaged laminated vein
S2 foliation
100 μm
f
Fine fracture
Apy
Au

shortening axes of these dextral and thrust faults suggest that they could be related to the same NNW–SSE shortening event (D_{NS}, Fig. 5c,d) already defined at Paddington, and are most likely explained as a result of minor and isolated re-orientations of regional ENE–WSW shortening between D_2 and D_4.

Yunndaga gold deposit

Geological setting

The Yunndaga gold deposit is located 6 km south of the Menzies township. The regional strike of the BTZ changes in this area from 350° to 330° (Fig. 1, Witt 1993; Hodkiewicz et al. 2005). Between 1897 and 1935, Yunndaga yielded approximately 8.75 t of gold (Witt 1992), and recent open pit operations (1995–1998) produced approximately 2.02 t of gold (Evans, unpublished). The NW-trending units at Yunndaga dip steeply to the SW, and comprise biotite-bearing sandstones with interbedded shale units, a minor layer of ultramafic schist, carbonaceous shale and a central mafic dolerite unit (Fig. 8). All of these rocks have been metamorphosed to lower amphibolite facies (Witt 1993; Beeson et al., unpublished). The southern section of the open pit has been back-filled with mine tailings, restricting descriptions here to its northern section.

Local deformation and gold mineralisation

The earliest deformation phase at Yunndaga is characterised by a NW-trending, steep westerly dipping pervasive foliation (Fig. 8). Similar to the BTZ gold deposits further south, this foliation is pronounced within the sandstone, shale and ultramafic units, and also at the dolerite contacts. In contrast to Paddington and New Boddington, stretching lineations plunge dominantly shallowly to the south (Fig. 8). The pervasive foliation is axial planar to moderately plunging symmetric folds and steeply plunging asymmetric and symmetric folds (Fig. 9a–c). No earlier foliations were observed within the fold hinge zones. Thus, asymmetric and symmetric folds are interpreted here to have formed during the same deformation event, and the variation in fold styles could be due to thickness variations and anisotropies within the sedimentary units, or due to a component of sinistral strike-slip motion during shortening and folding, causing fold rotation. There are a number of features, particularly well-developed within the sedimentary units, such as asymmetric, sigmoidal quartz grains, elongated parallel to the lineation (Fig. 9d), asymmetric sheared quartz veins showing sigmoidal shapes and fold asymmetries that suggest a sinistral component of strike-slip deformation parallel to the shallowly plunging lineation. Although resolving strike-slip deformation in arcuate shear zones is complex (Tikoff and Greene 1997; Lin and Jiang 2001), the mutual relationships between symmetrical and asymmetrical folds are most simply explained by the same ENE–WSW maximum shortening axis determined for the Paddington and New Boddington deposits and is typical of other regional shear systems within the EGP (Chen et al. 2001b).

Gold mineralisation is associated with a strike-parallel laminated vein located at the contact between the western margin of the dolerite and the quartz-rich sedimentary units (Fig. 8). Wall rock alteration is characterised by quartz–carbonate–biotite–chlorite–arsenopyrite–pyrrhotite–gold assemblages. Structural analysis of high-grade diamond drill core intersections (4 to 5 ppm Au) reveals that the laminated vein and associated wall rock sulphides are deformed and boudinaged by S_2. Similar to Paddington and New Boddington, visible gold is associated with fine fractures within arsenopyrite (Fig. 9e,f). As the trace of the laminated vein follows a NW-tending D_2 structure (Fig. 8), gold mineralisation has been interpreted to have formed during and consequently deformed by D_2.

Within the central and northern sections of the Yunndaga deposit, NE- and ENE-trending brittle–ductile faults (Fig. 8) cut across and offset all lithologies and earlier structures. These faults are not associated with a pervasive foliation, have sinistral lateral offset <10 m, cut across bedding and the axial planar foliation and reflect a later deformation event, associated with unmineralised quartz–carbonate veins within the dolerite unit. Slickenslide lineations along the ENE–WSW-trending faults vary from 40°–096° to 46°–071° and drag folding of the S_2 foliation and bedding indicate composite reverse-sinistral shearing. The brittle–ductile style and reverse-sinistral movement sense suggest a late and local anti-clockwise rotation of the D_2 maximum shortening axis towards a more northerly orientation.

Deformation and gold mineralisation within the BTZ

When compared to the regional shortening and gold mineralisation events of the EGP (i.e. D_1–D_4 of Table 1, Fig. 10a), the results from this study indicate that the BTZ is characterised by a simple structural evolution (Fig. 10b). Low-angle thrusting, recumbent folding and stacking of stratigraphy associated with N–S shortening is the first recognised shortening phase within the southern EGP (D_1, e.g. Gresham and Loftus-Hills 1981; Swager and Griffin 1990b). This style of deformation is typical of many greenstone-hosted orogenic gold deposits and shear systems (e.g. Hubert 1990; Milési et al. 1992; Robert and Poulsen 2001), but no evidence for it was found in the BTZ (Witt 1992, 1993; Beeson et al., unpublished). If the supracrustal

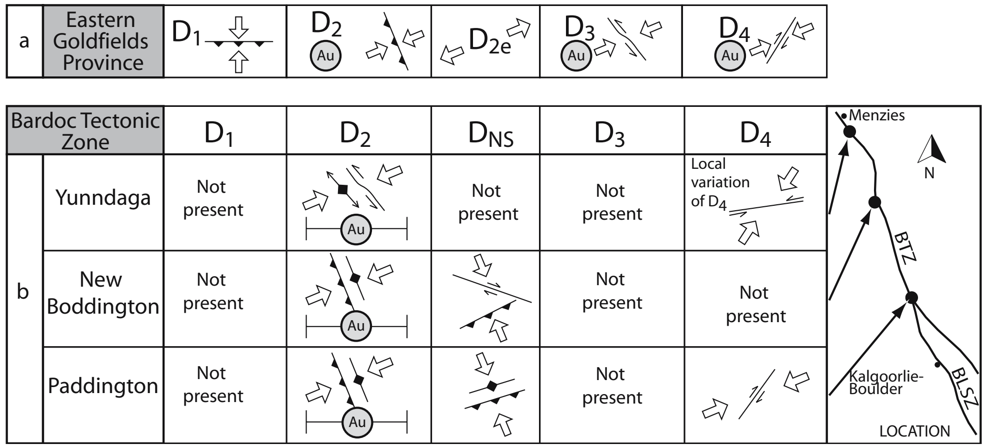

Fig. 10 Summary of the relative timing of deformation and gold mineralisation events within **a** The EGP and especially the BLSZ, and **b** From Paddington, New Boddington and Yunndaga. Note that D_{NS} is only a local deformation event observed at Paddington and New Boddington. Comparisons based on Swager (1997), Bateman and Hagemann (2004), Weinberg et al. (2003, 2005)

units that now define the BTZ did undergo D_1 deformation, any structures developed were likely rotated parallel to and overprinted by subsequent deformation events.

The first and most pervasive deformation event documented in all deposits is characterised by: (1) a steeply dipping, NNW-trending foliation axial planar to tight to isoclinal sub-horizontal folds, and (2) NNW-trending reverse/thrust shear systems. Together, these structures define a phase of intense crustal deformation related to ENE–WSW sub-horizontal shortening and sub-vertical extension along NNW-trending planes. The style and relative timing of this event is comparable to regional D_2 (Fig. 10; Swager and Griffin 1990b; Swager 1997; Weinberg et al. 2003).

In addition, D_2 at Yunndaga was associated with a component of sinistral strike-slip deformation along NW-trending planes. This is interpreted as a result of sinistral transpression during regional D_2, where the sinistral motion results from the change in strike of the BTZ in that area towards the NW (Fig. 1, cf. Hodkiewicz et al. 2005). An independent phase of D_3 sinistral strike-slip deformation is absent from the three deposits studied, which contrasts with Witt (1993, 1994) and other regional studies within the EGP (Swager 1997; Weinberg et al. 2003) where D_3 deformation was regarded as a major event. The lack of D_3 in the deposits studied could possibly be related to the geometrical constraints imposed by the large competent granite domes that bound this narrow corridor of supracrustal rocks. During regional ENE–WSW D_2 shortening, these granitic domes would have rotated the supracrustal rocks to their current orientation, roughly orthogonal to the maximum shortening direction (Fig. 1). Such an orientation would be unfavourable for reactivation of D_2 structures to strike-slip shearing.

Relatively late NE- and ENE-trending faults occur at Paddington and Yunndaga and at numerous other localities in the BTZ (Witt 1993, 1994). These structures are brittle–ductile in nature, represent the last deformation phase, have low offset magnitudes and, depending on their orientation, record oblique dip-slip to strike-slip movements (Witt 1993, Beeson et al., unpublished; this study). These faults can be readily correlated with the regional D_4 (Fig. 10).

In between D_2 and D_4, this study recorded structures at Paddington and New Boddington (Fig. 10b) derived from an inferred NNW-SSE sub-horizontal shortening axis. This deformation produced only relatively minor structures (sub-metric offsets, Figs. 5d, 7g), and they match those documented other by local- and regional-scale studies within the EGP (Ellis 1939; McMath 1953). Because of their minor offsets and localised nature, these structures are considered to be local variations of regional ENE–WSW shortening between regional D_2 and D_4.

Comparison to other major deposits and shear systems

The broad question underlying this study is why gold endowment within the BTZ (100 t Au) is an order of magnitude less than the BLSZ (>1,500 t Au), despite the two shear systems being physically linked along strike, cutting through similar rock packages and having had broadly the same geological history (Fig. 1). The BTZ deposits from this study are characterised by a common ore paragenesis comprised of carbonate, quartz, chlorite, muscovite, arsenopyrite and pyrite ± biotite (Morey, unpublished), but more importantly, our local studies show that veins and their gold-bearing sulphide assemblages are associated with and deformed by a major phase of ENE–WSW deformation (Figs. 3d,e, 7c and 9e), which corresponds with regional D_2 (Fig. 10). When applied to the whole shear system, this indicates that D_2 dominated the structural evolution and gold endowment history of the BTZ, which is characterised by uniform and intense reverse shearing and upright folding dispersed over a broad (>5 km across strike) deformation zone. Other regional (Witt 1993) and local (Colville et al. 1990; Alardyce and Vanderhor 1998) studies of the BTZ argued that gold mineralisation was controlled by strike-slip or oblique-slip faults related to D_3 and D_4, but as demonstrated by this work, these styles of deformation are either absent (D_3), or post-date (D_4) gold mineralisation. This is unlike a large number of gold camps in the EGP and elsewhere, where gold is related to either D_3 and D_4 (cf. Vearncombe 1998; Phillips et al. 1998; Ridley and Mengler 2000; Groves et al. 2000; Robert and Poulsen 2001; Micklethwaite and Cox 2004).

The deformation history of the BLSZ was more complex than that of the BTZ (Gresham and Loftus-Hills 1981; Swager and Griffin 1990b; Swager et al. 1995; Weinberg et al. 2005), where gold mineralisation was controlled by a greater variety of deformation styles and events (at least D_2–D_4, Fig. 10a,b, Bateman and Hagemann 2004; Nguyen et al. 1998; Ridley and Mengler 2000; Weinberg et al. 2005). The greater complexity in deformation and gold mineralisation is also reflected in the architecture of the BLSZ. This shear zone is a more tortuous, narrow (<2 km across strike; Micklethwaite and Cox 2004) shear system, linked to higher order, low offset splay structures in the vicinity of regional antiforms (Fig. 1; Hodkiewicz et al. 2005; Weinberg et al. 2005). These architectural characteristics are repeated in other richly endowed shear systems, such as the Abitibi Subprovince in Canada and the Ashanti gold belt in western Africa (e.g., Robert and Poulsen 1997, 2001; Milési et al. 1991). The giant Hollinger-McIntyre deposits of the Abitibi Subprovince in Canada are particularly noteworthy. Here, a large antiformal structure composed of mafic volcanic rocks is linked by higher order faults to the regional Porcupine-Destor Fault (Hodgson et al. 1990), which is very similar to the structural setting of the Golden Mile in the BLSZ (Fig. 1; Phillips et al. 1996). The competent, large antiformal structures provide more pronounced structural and lithological complexities, which are thought to give rise to regions of low mean stress and favour the formation of focussed, high permeability fluid systems that lead to large-scale gold deposition (Hodgson 1989; Ridley 1993; Ojala et al. 1993). In contrast, the BTZ does not contain any large-scale antiforms, or other favourable structural features such as secondary splay faults (Eisenlohr et al. 1989; Cox et al. 2001) or significant variations in strike of the shear system (Hodkiewicz et al. 2005) to promote host rock dilation and gold mineralisation. The most likely reason for the lack of geometrical and lithological complexities within the BTZ is that deformation was more intense within this broad shear system. More intense deformation explains the dominance of iso-clinal folds and pervasive reverse shear zones at Paddington, New Boddington and Yunndaga, and also why the majority of lithological contacts in map view are orthogonal to the regional ENE–WSW shortening direction, as opposed to the more variably striking features of the BLSZ system along strike to the south (Fig. 1).

The advantage of a more variable deformation history, as typified by richly endowed shear systems, is also demonstrated by geochronological studies within the Juneau gold belt of Alaska, USA, where a rapid release of mineralising fluids was associated with a switch in tectonic activity from orthogonal to transpressive shearing (Goldfarb et al. 1991). In contrast, the simple deformation history of the BTZ (Fig. 10b) would decrease the potential for the shear system to undergo switches in deformation events, which is more typical of the BLSZ and other richly endowed shear systems.

Although gold endowment is also dependent on other factors, such as the presence of gold-bearing hydrothermal fluids that can undergo sulphidation in a suitable physico-chemical environment, the key structural factors defined above help explain the lower gold endowment of the BTZ. Thus, variety of deformation events, developed within a lithologically and structurally complex, narrow shear system, all favour the gold endowment potential of an orogenic shear system.

Conclusions

As revealed by field studies from the Paddington, New Boddington and Yunndaga gold deposits, the structural history of the BTZ is dominated by intense D_2 shortening through the development of NNW-trending tight to iso-clinal folds and reverse to transpressive shear zones. This deformation event controlled the distribution of gold bearing structures within the BTZ, evident as syn-S_2 shear and stockwork veins, or conjugate planar vein arrays that mutually cross-cut and are overprinted by S_2. The BTZ is also characterised by a lack of evidence for other major deformation events (D_1, D_3), and although D_4 faulting is common, these structures consistently post-date gold mineralisation. This is in contrast with the highly endowed BLSZ immediately to the south along strike, where a more complex sequence of dip- and strike-slip deformation events (D_2, D_3 and D_4) are more well preserved and associated with gold mineralisation, and the shear system is characterised by a narrow (<2 km across strike), tortuous geometry in the vicinity of supracrustal units that preserve more complex geometries. Despite the possible influence of other physico-chemical factors, the comparatively simple structural and gold mineralisation evolution of the BTZ, when compared to the more complex BLSZ, helps explain the differences in gold endowment between these along strike shear systems.

Acknowledgment Research reported herein was released with permission of the CEO, *predictive mineral discovery**Cooperative Research Centre. Gerard Tripp, Scott Halley, Peter Sheehan, Robert Henderson and Darren Allingham of Placer Dome Asia Pacific (now Barrick Gold) are especially thanked for feedback and field assistance. Discussions with Caroline Forbes and Richard Blewett and constructive reviews by Jochen Kolb, Damien Gaboury, Richard Goldfarb, Georges Beaudoin (associate editor) and Larry Meinert (editor) are greatly appreciated for improving the quality of this manuscript. A. Morey acknowledges the support of a student travel grant awarded by the SGA to present the preliminary findings of this study at the 8th Biennial SGA Meeting, Beijing 2005.

References

Alardyce W, Vanderhor F (1998) Paddington. In: Vanderhor F, Groves DI (eds) Systematic documentation of Archaean gold deposits of the Yilgarn block. MERIWA Report no. 193, Part II, pp 115–119

Ames HG (1948) The Perron mine. Structural geology of Canadian ore deposits. Canadian Institute of Mining and Metallurgy, Geology Division, pp 893–898

Baggott MS, Vielreicher NM, Groves DI, McNaughton NJ (2005) Zircons, dykes and gold mineralization at Jundee-Nimray: post ca. 2.66 Ga Archean lode gold in the Yandal belt, Western Australia. Econ Geol 100:1389–1405

Bateman R, Hagemann SG (2004) Gold mineralisation throughout about 45 Ma of Archaean orogenesis; protracted flux of gold in the Golden Mile, Yilgarn Craton, Western Australia. Miner Depos 39:536–559

Blewett RS, Cassidy KF, Champion DC, Henson PA, Goleby BS, Jones L, Groenewald BP (2004) The Wangkathaa Orogeny: an example of episodic regional 'D2' in the late Archaean Eastern Goldfields Province, Western Australia. Precambrian Res 130:139–159

Bottomer LR, Robinson C (1990) Bardoc gold deposits. In: Hughes FE (ed) Geology of the mineral deposits of Australia and Papua New Guinea. Australasian Institute of Mining and Metallurgy, Melbourne, pp 385–388

Brown SM, Groves DI, Newton PGN (2002) Geological setting and mineralization model for the Cleo gold deposit, Eastern Goldfields Province, Western Australia. Miner Depos 37:704–721

Chen SF, Witt WK, Liu S (2001a) Transpression and restraining jogs in the northeastern Yilgarn Craton, Western Australia. Precambrian Res 106:309–328

Chen SF, Libby JW, Greenfield JE, Wyche S, Riganti A (2001b) Geometry and kinematics of large arcuate structures formed by impingement of rigid granitoids into greenstone belts during progressive shortening. Geology 29:283–286

Colville RG, Kelly D, Fish BL (1990) Goongarrie gold deposits. In: Hughes FE (ed) Geology of the mineral deposits of Australia and Papua New Guinea. Australasian Institute of Mining and Metallurgy, Melbourne, pp 363–366

Cox SF, Ruming K (2004) The St Ives mesothermal gold system, Western Australia—a case of golden aftershocks? J Struct Geol 26:1109–1125

Cox SF, Knackstedt MA, Braun J (2001) Principles of structural control on permeability and fluid flow in hydrothermal systems. Rev Econ Geol 14:1–24

Davis BK, Maidens E (2003) Archaean orogen-parallel extension: evidence from the northern Eastern Goldfields Province, Yilgarn Craton. Precambrian Res 127:229–248

Davis BK, Hickey KA, Rose S (2001) Superposition of gold mineralisation on pre-existing carbonate alteration; structural evidence from the Mulgarrie gold deposit, Yilgarn Craton. Aust J Earth Sci 48:131–149

Davis BK, Tripp GI, Trofimovs J, Archibald NJ (2007) Complexity of the structural-mineralization history in the Eastern Goldfields Province, Yilgarn Craton: evidence and implications from the study of gold mineralized systems. Economic Geology (in press)

Eisenlohr BN, Groves D, Partington GA (1989) Crustal-scale shear zones and their significance to Archaean gold mineralization in Western Australia. Miner Depos 24:1–8

Ellis HA (1939) The geology of the Yilgarn Goldfield south of the Great Eastern Railway. Geological Survey of Western Australia, Bulletin no. 97, Perth

Gaboury D, Carrier A, Crevier M, Pelletier C, Sketchley DA (2001) Predictive distribution of fault-fill and extensional veins; example from the Sigma gold mine, Abitibi Subprovince, Canada. Econ Geol 96:1397–1405

Gee RD (1975) Regional geology of the Archaean nuclei of the Western Australian Shield. In: Knight CL (ed) Economic geology of Australia and Papua New Guinea. Australasian Institute of Mining and Metallurgy, Monograph 5, pp 43–55

Goldfarb RJ, Snee LD, Miller LW, Newberry RJ (1991) Rapid dewatering of the crust deduced from ages of mesothermal gold deposits. Nature 354:296–298

Goldfarb RJ, Groves DI, Gardoll S (2001) Orogenic gold and geologic time; a global synthesis. Ore Geol Rev 18:1–75

Gresham JJ, Loftus-Hills GD (1981) The geology of the Kambalda nickel field, Western Australia. Econ Geol 76:1373–1416

Groves DI (1993) The crustal continuum model for late-Archaean lode-gold deposits of the Yilgarn Block, Western Australia. Miner Depos 28:366–374

Groves DI, Phillips GN, Ho SE, Houston SM, Standing CA (1987) Craton-scale distribution of Archean greenstone gold deposits: predictive capacity of the Metamophic Model. Econ Geol 82:2045–2058

Groves DI, Goldfarb RJ, Knox-Robinson CM, Ojala J, Gardoll S, Yun GY, Holyland P (2000) Late kinematic timing of orogenic gold deposits and significance for computer-based exploration techniques with emphasis on the Yilgarn Block, Western Australia. Ore Geol Rev 17:1–38

Hagemann SG, Cassidy KF (2000) Archean orogenic lode gold deposits. Rev Econ Geol 13:9–68

Hagemann SG, Cassidy KF (2001) World-class gold camps and deposits in the Eastern Goldfields Province, Yilgarn Craton: diversity in host rocks, structural controls, and mineralization styles. In: Hagemann SG, Neumayr P, Witt WK (eds) World-class gold camps and deposits in the eastern Yilgarn Craton, Western Australia, with special emphasis on the Eastern Goldfields Province. Geological Survey of Western Australia Record 2001/17, pp 7–44

Hammond RL, Nisbet BW (1992) Towards a structural and tectonic framework for the central Norsenman-Wiluna greenstone belt, Western Australia. Proceedings volume for the Third International Archaean Symposium, Geology Department (Key Centre) and University Extension Publication No. 22, pp 39–49

Hancock MC, Robertson IG, Booth GW (1990) Paddington gold deposits. In: Hughes FE (ed) Geology of the mineral deposits of Australia and Papua New Guinea. Australasian Institute of Mining and Metallurgy, Melbourne, pp 395–400

Hodgson CJ (1989) The structure of shear-related, vein-type gold deposits: a review. Ore Geol Rev 4:231–273

Hodgson CJ, Hamilton JV, Piroshco DW (1990) Structural setting of gold deposits and the tectonic evolution of the Timmins-Kirkland Lake area, southwestern Abitibi greenstone belt. In: Ho SE, Robert F, Groves DI (eds) Gold and base-metal mineralization in the Abitibi Subprovince, Canada, with emphasis on the Quebec segment. The University of Western Australia Publication No. 24, Geology Department (Key Centre) and the University Extension, pp 101–120

Hodkiewicz PF, Weinberg RF, Gardoll SJ, Groves D (2005) Complexity gradients in the Yilgarn Craton: fundamental controls on crustal-scale fluid flow and the formation of world-class orogenic-gold deposits. Aust J Earth Sci 52:831–841

Hubert C (1990) Geologic framework, evolution and structural setting of gold and base metal deposits of the Abitibi greenstone belt, Canada. In: Ho SE, Robert F, Groves DI (eds) Gold and base–

metal mineralization in the Abitibi Subprovince, Canada, with emphasis on the Quebec segment. The University of Western Australia, Geology Department (Key Centre) and the university extension Publication No. 24, pp 53–62

Hunter WM (1993) Geology of the granite–greenstone terrane of the Kalgoorlie and Yilma 1:100,000 sheets, Western Australia. Geological Survey of Western Australia, Report 35

Kretz R (1983) Symbols for rock-forming minerals. Am Mineral 68:277–279

Lin S, Jiang D (2001) Using along-strike variation in strain and kinematics to define the movement direction of curved transpressional shear zones; an example from northwestern Superior Province, Manitoba. Geology 29:767–770

McMath JC (1953) The geology of the country about Coolgardie, Coolgardie Goldfield, WA. Geological Survey of Western Australia Bulletin 107

Micklethwaite S, Cox SF (2004) Fault-segment rupture, aftershock-zone fluid flow, and mineralization. Geology 32:813–816

Milési JP, Ledru P, Ankrah P, Johan V, Marcoux E, Vinchon C (1991) The metallogenic relationship between Birimian and Tarkwaian gold deposits in Ghana. Miner Depos 26:228–238

Milési JP, Ledru P, Feybesse J-L, Dommanget A, Marcoux E (1992) Early Proterozoic ore deposits and tectonics of the Birimian orogenic belt, West Africa. Precambrian Res 58:305–344

Myers JS (1993) Precambrian history of the West Australian Craton and adjacent orogens. Annu Rev Earth Planet Sci 21:453–485

Nelson DR (1998) Compilation of SHRIMP U–Pb zircon geochronology data, 1997. Geological Survey of Western Australia Record 1998/2, Perth

Nelson DR (2002) Compilation of geochronology data 2001. Geological Survey of Western Australia Record 2002/2, Perth

Nguyen TP, Cox SF, Harris LB, Powell CM (1998) Fault-valve behaviour in optimally oriented shear zones: an example at the Revenge Mine, Kambalda, Western Australia. J Struct Geol 20:1625–1640

Ojala VJ, Ridley JR, Groves DI, Hall GA (1993) The Granny Smith gold deposit: the role of heterogeneous stress distribution at an irregular granitoid contact in a greenschist facies terrane. Miner Depos 28:409–419

Passchier CW (1994) Structural geology across a proposed Archaean terrane boundary in the eastern Yilgarn Craton, Western Australia. Precambrian Res 68:43–64

Phillips GN, Groves DI, Kerrich R (1996) Factors in the formation of the giant Kalgoorlie gold deposit. Ore Geol Rev 10:295–317

Phillips GN, Vearncombe JR, Eshuys E (1998) Yandal greenstone belt, Western Australia: 12 million ounces of gold in the 1990s. Miner Depos 33:310–316

Ransted TW (1990) Eureka gold deposit. In: Hughes FE (ed) Geology of the mineral deposits of Australia and Papua New Guinea. Australasian Institute of Mining and Metallurgy, Melbourne, pp 383–384

Ridley JR (1993) The relations between mean rock stress and fluid flow in the crust: with reference to vein- and lode-style gold deposits. Ore Geol Rev 8:23–37

Ridley JR, Mengler F (2000) Lithological and structural controls on the form and setting of vein stockwork orebodies at the Mount Charlotte gold deposit, Kalgoorlie. Econ Geol 95:85–98

Robert F, Brown AC (1986) Archean gold-bearing quartz veins at the Sigma Mine, Abitibi greenstone belt, Quebec; Part II, Vein paragenesis and hydrothermal alteration. Econ Geol 81:593–616

Robert F, Poulsen KH (1997) World-class Archaean gold deposits in Canada; an overview. Aust J Earth Sci 44:329–351

Robert F, Poulsen KH (2001) Vein formation and deformation in greenstone gold deposits. In: Richards JP, Tosdal RM (eds) Structural controls on ore genesis. Rev Econ Geol 14:111–155

Ross AA, Barley ME, Brown SJA, McNaughton NJ, Ridley JR, Fletcher IR (2004) Young porphyries, old zircons: new constraints on the timing of deformation and gold mineralisation in the Eastern Goldfields from SHRIMP U–Pb zircon dating at the Kanowna Belle Gold Mine, Western Australia. Precambrian Res 128:105–142

Salier BP, Groves DI, McNaughton NJ, Fletcher IR (2004) The world-class Wallaby gold deposit, Laverton, Western Australia; an orogenic-style overprint on a magmatic-hydrothermal magnetite–calcite alteration pipe? Miner Depos 39:473–494

Salier BP, Groves DI, McNaughton NJ, Fletcher IR (2005) Geochronological and stable isotope evidence for widespread orogenic gold mineralization from a deep-seated fluid source at ca. 2.65 Ga in the Laverton Gold Province, Western Australia. Econ Geol 100:1363–1388

Swager CP (1997) Tectono-stratigraphy of late Archaean greenstone terranes in the southern Eastern Goldfields, Western Australia. Precambrian Res 83:11–42

Swager CP, Griffin TJ (1990a) Geology of the Archaean Kalgoorlie terrane, northern and southern sheets, 1: 250 000. Geological Survey of Western Australia, Perth

Swager CP, Griffin TJ (1990b) An early thrust duplex in the Kalgoorlie-Kambalda greenstone belt. Precambrian Res 48:63–73

Swager CP, Griffin TJ, Witt WK, Wyche S, Ahmat AL, Hunter WM, McGoldrick PJ (1995) Geology of the Archaean Kalgoorlie Terrane—an explanatory note (reprint of Record 1990/12). Geological Survey of Western Australia Report 48

Tikoff B, Greene D (1997) Stretching lineations in transpressional shear zones: an example from the Sierra Nevada Batholith, California. J Struct Geol 19:29–39

Tremblay A (2001) Postmineralization faults in the Beaufor gold deposit, Abitibi greenstone belt, Canada: geometry, origin, and tectonic implications for the Val-d'Or mining district. Econ Geol 96:509–524

Vearncombe JR (1998) Shear zones, fault networks, and Archean gold. Geology 26:855–858

Weinberg RF, Moresi L, Van der Borgh P (2003) Timing of deformation in the Norseman-Wiluna Belt, Yilgarn Craton, Western Australia. Precambrian Res 120:219–239

Weinberg RF, Van der Borgh P, Bateman R, Groves D (2005) Kinematic history of the Boulder-Lefroy Shear Zone System and controls on associated gold mineralization, Yilgarn Craton, Western Australia. Econ Geol 100:1407–1426

Whitaker AJ, Bastrakova IV (2002) Yilgarn Craton Aeromagnetic interpretation. 1:1 500 000 scale map. Geoscience Australia

Williams IR (1974) Structural subdivision of the Eastern Goldfiels Province, Yilgarn Block. Geological Survey of Western Australia, Annual Report, pp 53–59

Witt WK (1992) Gold deposits of the Menzies and Broad Arrow areas, Western Australia. Part 1 of a systematic study of the gold mines of the Menzies–Kambalda region. Geological Survey of Western Australia Record 1992/13

Witt WK (1993) Gold mineralisation of the Menzies-Kambalda Region, Eastern Goldfields, Western Australia. Geological Survey of Western Australia, Report 39

Witt WK (1994) Geology of the Bardoc 1:100 000 sheet. Geological Survey of Western Australia, pp 50

Witt WK, Swager CP (1989) Structural setting and geochemistry of Archaean I-type granites in the Bardoc-Coolgardie area of the Norseman-Wiluna Belt, Western Australia. Precambrian Res 44:323–351

Yeats CJ, McNaughton NJ, Ruettger D, Bateman R, Groves DI, Harris JL, Kohler E (1999) Evidence for diachronous Archean lode gold mineralization in the Yilgarn Craton, Western Australia: a SHRIMP U–Pb study of intrusive rocks. Econ Geol 94:1259–1276

Yeats CJ, Kohler EA, McNaughton NJ, Tkatchyk LJ (2001) Geological setting and SHRIMP U–Pb geochronological evidence for ca. 2680–2660 Ma lode-gold Mineralization at Jundee-Nimray in the Yilgarn Craton, Western Australia. Miner Depos 36:125–136